ChemComm

COMMUNICATION

View Article Online
View Journal

Cite this: DOI: 10.1039/c5cc05722a

Received 10th July 2015,
Accepted 22nd October 2015

DOI: 10.1039/c5cc05722a

www.rsc.org/chemcomm

Unusually high thermal stability and peroxidase activity of cytochrome *c* in ionic liquid colloidal formulation†

Pankaj Bharmoria[a] and Arvind Kumar*[ab]

Ionic liquid (IL) surfactant choline dioctylsulfosuccinate, [Cho][AOT], formed polydispersed vesicular structures in the IL, ethylmethylimidazolium ethylsulfate, [C_2mim][C_2OSO_3]. Cytochrome *c* dissolved in such a colloidal medium has shown very high peroxidase activity (~2 times to that in neat IL and ~4 times to that in an aqueous buffer). Significantly, the enzyme retained both structural stability and functional activity in IL colloidal solutions up to 180 °C, demonstrating the suitability of the system as a high temperature bio-catalytic reactor.

Synthetic vesicular membranes have long been used as mimics to understand the phospholipid bio-membranes synergy with proteins.[1–3] The vesicles are colloidal bilayer architectures formed by surfactants upon aggregation beyond the critical aggregation concentration.[4] In living systems, the protein-biomembrane synergy performs key functions like cell metabolism, signalling, and cell gatekeeping and also act as drugs targets.[1] This synergy has been mimicked *in vitro* for commercial utility with synthetic surfactants as protein–surfactant colloidal formulations in pharmaceuticals, cosmetics, drug delivery, biochemical reactions, and very recently in bioelectronics.[5] However, most of these formulations are restricted to aqueous medium within the range of room temperature operation.

The rise of ionic liquids (ILs—salts with melting points <100 °C[6]) as thermally stable green solvents liaising with an accessible solvating ability and surface activity has generated new opportunities to utilize them as a medium for the preservation of biomolecules and to develop thermally stable surfactant–protein colloidal formulations. However, there are several hurdles in the formulation of such colloidal systems in an IL medium due to (i) the limited solubility of proteins[7] and surfactants, particularly the anionic surfactants,[8] (ii) the high probability of structural alterations and functional deactivation of proteins,[9] and (iii) the poor/weak self-assembly of surface active molecules. Despite these limitations, some ILs have been found suitable to dissolve proteins with a slightly perturbed structure with the retention of functional activity[10] and the ability to support the self-assembly of a variety of amphiphiles.[11] There are a few reports of supramolecular assemblies, such as "vesicles" of surfactants, lipids, or block copolymers, in an IL medium.[12] However, no report is yet available wherein both the protein and surfactant could be dissolved in a common IL, and therefore, the binding behavior of proteins with surfactants or surfactant-like ILs in an IL medium is completely unexplored.

Guided by the work of Malvika Bihari *et al.*,[10] wherein cytochrome *c* (Cyt *c*) could be homogeneously dissolved in [C_2mim][C_2OSO_3] with the retention of peroxidase activity at room temperature and our own previous work on the formation of vesicles and reverse vesicles of an IL surfactant in an IL medium,[13] herein we report a novel colloidal formulation comprising Cyt *c*-[Cho][AOT]–[C_2mim][C_2OSO_3] as the constituent. The experimental details, materials, and dissolution characteristics of Cyt *c* in [Cho][AOT]–[C_2mim][C_2OSO_3] are provided in Fig. S1–S5 (ESI†).

Initially, we characterised the self-assembling behaviour of [Cho][AOT] in [C_2mim][C_2OSO_3] medium from the I_1/I_3 vibronic band ratio of pyrene as the polarity probe, Fig. 1A, and using isothermal titration calorimetry (ITC), Fig. 1B.

The I_1/I_3 ratio (1.20) of pyrene in the native [C_2mim][C_2OSO_3] lies between highly non-polar and polar solvents and therefore, indicates the presence of various bicontinuous microphases comprising polar/non-polar domains.[14] Two transitions can be observed in Fig. 1A. The first transition at 5.5 mmol L^{-1} (CAC_1) corresponds to the formation of pre-vesicular aggregates, wherein some of the [C_2mim][C_2OSO_3] molecules remain embedded in the aggregates of [Cho][AOT]. Above 5.5 mmol L^{-1}, the I_1/I_3 ratio increases a bit before decreasing in a sigmoidal fashion before becoming constant in the post-aggregation region. The constancy of the I_1/I_3 ratio indicates that pyrene senses a uniform hydrophobic environment in the [Cho][AOT] aggregates. The second

[a] *AcSIR, CSIR-Central Salt and Marine Chemicals Research Institute, Bhavangar-364002, India*
[b] *Salt and Marine Chemicals Division, CSIR-Central Salt and Marine Chemicals Research Institute, Bhavnagar-364002, India. E-mail: arvind@csmcri.org; Fax: + 91-278-2567562; Tel: +91-278-2567039*

† Electronic supplementary information (ESI) available: Materials, methods, purity specifications (Table S1) and experimental details (Fig. S1–S5), equations used are given as annexure-I, detailed results. See DOI: 10.1039/c5cc05722a

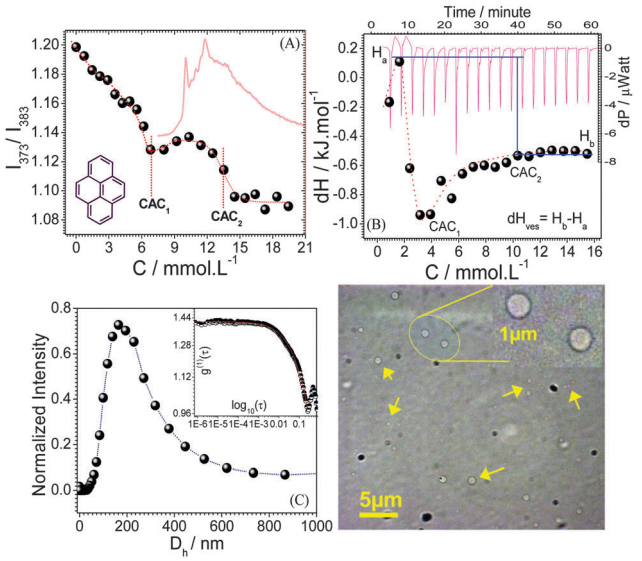

Fig. 1 (A) Pyrene I_1/I_3 *vs.* [Cho][AOT] conc. Curve along with the fluorescence spectra of pyrene in $[C_2mim][C_2OSO_3]$, shown as the inset. (B) Isothermal titration calorimetric plot of [Cho][AOT] dilution in $[C_2mim][C_2OSO_3]$, with the d*P* plot as the inset. (C) D_h plot with corresponding autocorrelation function as the inset. (D) Optical images of [Cho][AOT] vesicles in $[C_2mim][C_2OSO_3]$ medium (the black spots in the figure are due to lens artefacts).

transition observed at 13.52 mmol L^{-1} corresponds to the critical vesicular concentration (CAC_2). Such an aggregation behavior has been previously observed for CTAB in $[C_6mim]Br/H_2O$ and $[C_4mim]Br/H_2O$ mixtures.[15]

The ITC curve (Fig. 1B) also confirms the aggregation of [Cho][AOT] in the $[C_2mim][C_2OSO_3]$ medium. The negative enthalpy changes observed from the enthalpogram indicates that in the aggregation process of [Cho][AOT], van der Waal's interactions dominate over the electrostatic interactions between [Cho][AOT] and $[C_2mim][C_2OSO_3]$.[13] It is to be noted that the Gordon parameter (*G*), an indicator of the solvophobic effect of a solvent to support self-assembly, is 0.846 for $[C_2mim][C_2OSO_3]$,[11a] which is higher than the 0.463 of $[C_4mim][Tf_2N]$ reported earlier to support the self-assembly of $[ProC_3][LS]$.[13] Therefore, the good solvophobicity of $[C_2mim][C_2OSO_3]$ can be accounted as one of the reasons to support the self-assembly of [Cho][AOT]. The Gibbs free energy of aggregation, ΔG°_{agg}, (−14.4 kJ mol^{-1}) was calculated using the mass action model (Annex 1, ESI†) by considering the ionisation degree of aggregation (α) as 1 due to the exclusively ionic shell surrounding the aggregates in the IL medium. A negative value of ΔG°_{agg} indicates the feasibility of [Cho][AOT] self-assembly in $[C_2mim][C_2OSO_3]$. The entropic contribution $\left(T\Delta S^\circ_{agg}\right)$ to the ΔG°_{agg} was determined from the standard Gibbs free energy equation (Annex 1, ESI†) and was found to be 14.82 kJ mol^{-1}. The high $T\Delta S^\circ_{agg}$ value compared to ΔH°_{agg} (−0.42 kJ mol^{-1}) indicates that the aggregation process is mainly entropy driven.

The formation of aggregated structures was confirmed from DLS measurements (Fig. 1C). The hydrodynamic diameter (D_h) of the [Cho][AOT] (50 mmol L^{-1}) aggregates in the $[C_2mim][C_2OSO_3]$ medium at a scattering angle of 90° and at 298.15 K was found to be 164 nm, which is comparable to that of [Cho][AOT] vesicles in water (150 nm).[16] Upon comparing the intensity autocorrelation function of the scattered light by [Cho][AOT] aggregates in $[C_2mim][C_2OSO_3]$ and aqueous medium (Fig. S6, ESI†), it was found that the decay time (τ) in $[C_2mim][C_2OSO_3]$ (τ = 1.63 ms) is two order of magnitude higher than that in water (τ = 17.6 μs). Slow relaxation of the scattered light in $[C_2mim][C_2OSO_3]$ can possibly be accounted for due to its high viscosity (97.58 cP compared to 0.890 cP of water at 25 °C).[17] In sight of a more transparent understanding of the *in situ* aggregate size, we performed multi-angle DLS measurements from 30° to 150° (Fig. S7, ESI†). The hydrodynamic diameter D_h increased from 130 nm to 600 nm as the angle varied from 30° to 150°, thus indicating the polydispersed nature of the aggregates. In order to reveal the morphology of the [Cho][AOT] aggregates in $[C_2mim][C_2OSO_3]$ medium, we performed optical microscopy (Fig. 1D and Fig. S8, ESI†). The microscopy images showed spherical droplets in the size range of 0.1–1 μm. The droplets observed are the polydispersed vesicles. Similar observation of formation of vesicles of an IL in an IL medium was reported by us in our previous communication (*Chem. Commun.*, 2013).[13] [Cho][AOT] self-assemblies in $[C_2mim][C_2OSO_3]$ were found to be kinetically stable at room temperature as no precipitation or phase separation was observed for 10 months, even at a concentration as high as 300 mmol L^{-1}. The proposed structure of the [Cho][AOT] vesicles in $[C_2mim][C_2OSO_3]$ medium is depicted in Fig. S9 (ESI†).

We explored the application of [Cho][AOT]–$[C_2mim][C_2OSO_3]$ colloidal system as a high temperature preservative for the enzyme Cyt *c* by investigating its binding behavior, conformational stability, and functional activity. The binding isotherm of [Cho][AOT] to Cyt *c* (15 μM) dissolved in $[C_2mim][C_2OSO_3]$ (Fig. 2A) was defined by subtracting the dilution enthalpogram of [Cho][AOT] in $[C_2mim][C_2OSO_3]$ medium from that of Cyt *c*-$[C_2mim][C_2OSO_3]$ solution (Fig. S10, ESI†). In surfactant–protein systems, the surfactant interacts with protein in different forms (monomers at low concentration, protein-induced aggregates in the mid-concentration region, and as micelle or vesicles, post CAC).[18] The binding of [Cho][AOT] to Cyt *c* at low concentration is an endothermic process, whereas the binding of [Cho][AOT], aggregates, and vesicles to cytochrome is an exothermic process with a small change in enthalpy. It is to be noted that small enthalpy changes upon binding to proteins occur when the interactions are electrostatic in nature.[19] Therefore, the small enthalpy changes indicate that [Cho][AOT] binds to Cyt *c* mainly through electrostatic interactions.[19]

Alterations in the structure of Cyt *c* upon [Cho][AOT] binding at different concentrations were measured from the changes in UV-Vis spectra (Fig. 2B). In the neat $[C_2mim][C_2OSO_3]$, Cyt *c* showed an intense Soret band at 408 nm and weak Q bands at 528 and 556 nm due to π–π* transitions in the heme group buried deep inside the hydrophobic core of the protein.[10a] Upon the addition of [Cho][AOT], a slight increase in absorbance of Cyt *c* was observed in low concentrations, followed by a continuous decrease in absorbance at higher concentrations. The decrease in absorbance (hypsochromic shift) occurs due to the lowering in

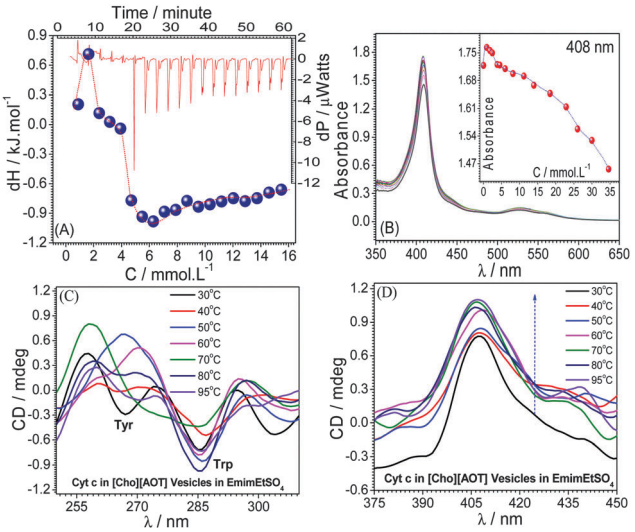

Fig. 2 (A) Binding isotherm of [Cho][AOT] binding to Cyt *c* (15 μM) in neat $[C_2mim][C_2OSO_3]$; (B) UV-Vis spectra of Cyt *c* (15 μM) in different [Cho][AOT] concentrations; (C and D) Mid-UV CD spectra of Cyt *c* in [Cho][AOT] (100 mM) + $[C_2mim][C_2OSO_3]$.

energy of the π* orbital upon exposure to the surrounding polar environment, which is possible due to the unfolding of the protein around the heme cleft. Though an unfolding was observed around the heme cleft, unlike the aqueous formulation, the oxidation state of Cyt *c* did not change at any concentration, as indicated by the retention of Q bands at 528 and 556 nm. Due to the absorption of imidazolium in the far UV-region, we could not observe the secondary structure of Cyt *c* from the CD-measurements. However, when we compared the mid-UV CD spectra, the bands due to Tyr and Trp were observed at 263 and 287 nm, but the Phe band was missing (Fig. S11, ESI†). Therefore, compared to water, the Tyr and Trp residues experienced a more non-polar environment, which can be due to the presence various non-polar domains in $[C_2mim][C_2OSO_3]$.[14] Upon the addition of 100 mM [Cho][AOT], a bathochromic shift of 4 nm in the band at 263 nm and a hypsochromic shift of 2 nm in the band at 287 was observed; this indicated that the conformation of the protein in the vesicles is such that Trp, which is present around the heme pocket, faces the hydrophobic tail part of the vesicle. The rise in ellipsity (θ) of the Tyr and Trp residues indicated the stabilisation of the tertiary structure of the protein.

We also checked the thermal stability of Cyt *c* in the vesicular regime by measuring the temperature-dependent CD spectra of the Tyr and Trp residues (Fig. 2C) and the Soret band at 408 nm (Fig. 2D). The band due to Tyr at 267 nm disappeared with the rise in temperature, which indicated conformational changes in the protein backbone, as three of the Tyr residues are usually present in the protein backbone. The overall θ of the bands (at 286 nm due to Trp and the Soret band at 408 nm) increased with their respective signs upon increasing the temperature from 30 to 95 °C without deformation of the CD bands, which indicated the thermal stability of the protein's tertiary structure in the region around the heme cleft. Because of the inbuilt temperature limitations of CD and UV-Vis spectrophotometers, the measurements above 100 °C were carried out by heating the samples outside the spectrophotometer using a silicon oil bath. The CD and UV-Vis spectra of the incubated samples were then obtained. The comparative CD and UV-Vis spectra of Cyt *c* dissolved in $[C_2mim][C_2OSO_3]$ and [Cho][AOT]–$[C_2mim][C_2OSO_3]$ measured at different temperatures and time periods are provided in Fig. S12 and S13 (ESI†). Retention of the CD Soret band at 408 nm and the UV Soret and Q bands indicated the structural stabilisation of Cyt *c* around the heme cleft. It has been observed that Cyt *c* remains stable up to 180 °C for a maximum of 5 min, whereas at 130 °C it remains stable for a time period of 1 h. These conclusions were arrived at by checking the structural stabilisation of Cyt *c* for more than 1 h at 130 °C and for 1 h at 140 °C, wherein Cyt *c* was found to lose its activity. It has also been observed that the time period for structural stabilisation of Cyt *c* increased with the decrease in temperature, as evident from its spectra at 100 °C after 6 h of heating (Fig. S12A, B and S13A, ESI†). Comparison of the stabilisation of Cyt *c* in $[C_2mim][C_2OSO_3]$ and [Cho][AOT]–$[C_2mim][C_2OSO_3]$ solutions showed that Cyt *c* remains more stable in water, which is evident from the higher ellipsity of the CD Soret band at 408 nm (Fig. S12, ESI†) and the higher absorbance of the UV Soret and Q bands (Fig. S13, ESI†). Therefore, the [Cho][AOT] vesicles imparted extra thermal stability to Cyt *c* in the colloidal formulation.

The activity of Cyt *c* (30 μM) in $[C_2mim][C_2OSO_3]$ or [Cho][AOT]–$[C_2mim][C_2OSO_3]$ was investigated by incubating the Cyt *c* solutions for 10 min in the temperature range from 60 to 180 °C. After incubation, the catalytic activity was observed using guaiacol as a substrate and H_2O_2 as an oxygen donor at room temperature. Cyt *c* catalyses the oxidation of guaiacol to tetraguaiacol, giving an orange colour and showing an absorption band at 470 nm (Fig. S14 and S15, ESI†).[20] Qualitatively, the activity was monitored by visual inspection of the appearance of the orange colour (Fig. 3).

Cyt *c* retained its functional activity up to 180 °C for a maximum of 5 min and 160 °C for a maximum of 10 min, both in neat $[C_2mim][C_2OSO_3]$ and [Cho][AOT]–$[C_2mim][C_2OSO_3]$ vesicular solution. 180 °C is considered as the highest activity temperature on account of the fact that the maximum product formation occurs within five minutes of the reaction inception (Fig. S16, ESI†). Quantitatively, the tetraguaiacol formation was calculated from the absorption changes at 470 nm and the molar extinction coefficient of 2.66×10^4 $cm^{-1}.M^{-1}$ (Fig. S17, ESI†). The activity of Cyt *c* in the [Cho][AOT]–$[C_2mim][C_2OSO_3]$ vesicular solutions was found to be ~2-fold higher than that observed in neat $[C_2mim][C_2OSO_3]$ at all temperatures (Fig. S18A, ESI†).

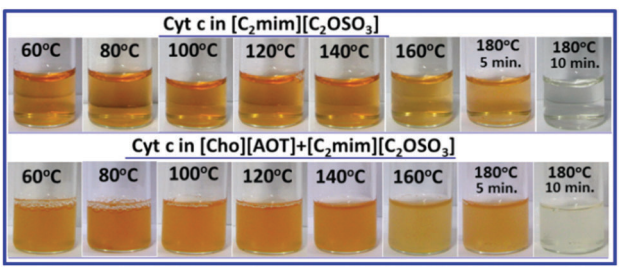

Fig. 3 Functional activity of Cyt *c* in $[C_2mim][C_2OSO_3]$ and [Cho][AOT](100 mM)–$[C_2mim][C_2OSO_3]$ from 60 to 180 °C.

The higher activity in vesicular solution can be attributed to (i) exposure of the catalytic iron centre of the enzyme due to a slight perturbation in conformation around the heme cleft[10a] as observed from the UV-Vis and CD spectra (Fig. 2B–D), (ii) the higher thermal stability imparted by [Cho][AOT] vesicles in the [Cho][AOT]–[C_2mim][C_2OSO_3] system (Fig. S12 and S13, ESI†). Since Cyt *c* retained its activity in buffer solution until 80 °C, we did a comparative analysis of the activity of Cyt *c* in buffer, in neat [C_2mim][C_2OSO_3] and in [Cho][AOT] (100 mM)–[C_2mim][C_2OSO_3] vesicular solutions by incubating the enzyme at 80 °C (Fig. S18B, ESI†). It was found that the activity of Cyt *c* in [Cho][AOT]–[C_2mim][C_2OSO_3] vesicular solution after 5 min of incubation is ~4 fold higher than in buffer and ~2-fold higher than in neat [C_2mim][C_2OSO_3]. The initial rates of enzymatic reactions were calculated from the maxima of the first derivatives of the product formation curve ($r = d(P)/dt$). Due to the technical limitation of the UV-Vis instrument to detect the absorbance changes below 0.5 min, we extrapolated the product formation curve to its zero value in order to calculate the initial rate of reaction. It was found that the initial rate of enzymatic reaction in [Cho][AOT]–[C_2mim][C_2OSO_3] solutions (158.8 μM min^{-1}) is 4-fold higher than that in neat [C_2mim][C_2OSO_3] (39.2 μM min^{-1}) and 13-fold higher than in buffer (12.17 μM min^{-1}). A high activity of Cyt *c* has earlier been reported in ILs ([C_4mim][Tf_2N], [C_4mim][PF_6] and in [C_8mim][PF_6]) solutions of methanol/crown ether at 40 °C with the addition of pyridine.[21] The higher activity of Cyt *c* herein can also be accounted for by the greater number of collisions of the substrate and the exposed catalytic iron centre of Cyt *c*. The vesicles provide a suitable water-vesicle interface with a large interfacial area to increase the contact between substrate and enzyme active sites, similar to that observed for micellar catalysis by enzymes in ILs.[22] The redox activity of Cyt *c* was also analysed at a maximum temperature (130 °C) of stabilisation for 1 h and at 100 °C for 6 h, wherein Cyt *c* was found to be redox active (Fig. S19, ESI†). Such a redox activity has previously been reported by Tamura *et al.* in the IL [Amim][Cl] in the temperature range from 120 to 140 °C for 3 h using optical-waveguide (OWG) spectroscopy. The authors cited the importance of polar ILs with hydrogen bond basicity, $\beta > 0.7$, as one of the reason for protein solubilisation and stabilisation.[23] β of [C_2mim][C_2OSO_3] is 0.71 and therefore must be one of the reasons for Cyt *c* solubilisation and stabilisation. Furthermore, the decrease in stabilisation time with temperature can be accounted for by the thermal stability of [C_2mim][C_2OSO_3] with a flash point of 162 °C, and thereafter a slow degradation of the [C_2OSO_3] anion begins to happen,[24] thus introducing the volume effects towards structural and functional stability.

It has been shown that [C_2mim][C_2OSO_3] is a unique IL, which can dissolve the enzyme Cyt *c* with slight conformational alterations and can also support the self-assembly of the anionic surface active IL [Cho][AOT] in the form of vesicles. The hydrogen bond basicity, $\beta = 0.71$, and good solvophobicity ($G = 0.846$) of [C_2mim][C_2OSO_3] can be accounted for as reasons for Cyt *c*'s solubility and [Cho][AOT] self-assembly in [C_2mim][C_2OSO_3]. Cyt *c* thus dissolved in [Cho][AOT]–[C_2mim][C_2OSO_3] vesicular solutions retains its functional activity up to very high temperatures for different time periods. The results demonstrate the potential of IL colloidal solutions as media for the preservation of enzymes and as enzymatic catalytic reactors at elevated temperatures.

Financial support from DST, India for this work (No. SB/S1/PC-104/2012) is acknowledged. We thank the Centralized Instrumental Facility, Dr. Santlal Jaiswar, Praveen Singh Gehlot and Damarla Krishnaiah for assistance in various capacities.

Notes and references

1 U. H. N. Dürr, M. Gildenberg and A. Ramamoorthy, *Chem. Rev.*, 2012, **112**, 6054–6074.
2 M. N. Jones, *Chem. Soc. Rev.*, 1992, **21**, 127–136.
3 E. Soussan, S. Cassel, M. Blanzat and I. Rico-Lattes, *Angew. Chem., Int. Ed.*, 2009, **48**, 274–288.
4 J. N. Israelachvili, *Intermolecular and Surface Forces*, Academic Press, New York, 1992.
5 K. P. Ananthapadmanabhan and E. D. Goddard, *In Interactions of Surfactants with Polymers and Proteins*, CRC Press, Inc, London, UK, 1993, ch. 8.
6 *Green Industrial Applications of Ionic Liquids*, ed. R. D. Rogers, K. R. Seddon and S. Volkov, NATO Science Series, Kluwer, Dordrecht, 2002.
7 R. M. Lau, M. J. Sorgedrager, G. Carrea, F. van Rantwijk, F. Secundo and R. A. Sheldon, *Green Chem.*, 2004, **6**, 483–487.
8 M. Moniruzzaman, N. Kamiya, K. Nakashima and M. Goto, *Chem-PhysChem*, 2008, **9**, 689–692.
9 R. M. Vrikkis, K. J. Fraser, K. Fujita, D. R. MacFarlane and G. D. Elliott, *J. Biomech. Eng.*, 2009, **131**, 074514.
10 M. Bihari, T. P. Russell and D. A. Hoagland, *Biomacromolecules*, 2010, **11**, 2944–2978; N. Byrne, L. M. Wang, J. P. Belieres and C. A. Angell, *Chem. Commun.*, 2007, 2714–2716; D. Constatinescu, C. Herrmann and H. Weingartner, *Phys. Chem. Chem. Phys.*, 2010, **12**, 1756–1763; J. P. Mann, A. McCluskey and R. Atkin, *Green Chem.*, 2009, **11**, 785–792; N. Byrne, J. P. Belieres and C. A. Angell, *Aust. J. Chem.*, 2009, **62**, 328–333; K. Tamura, N. Nakamura and H. Ohno, *Biotechnol. Bioeng.*, 2012, **109**, 729–735.
11 (*a*) T. L. Greaves and C. J. Drummond, *Chem. Soc. Rev.*, 2013, **42**, 1096–1120; (*b*) B. Fernández-Castro, T. Méndez-Morales, J. Carrete, E. Fazer, O. Cabeza, J. R. Rodríguez, M. Turmine and L. M. Varela, *J. Phys. Chem. B*, 2011, **115**, 8145–8154; (*c*) L. Shi and L. Zheng, *J. Phys. Chem. B*, 2012, **116**, 2162–2172.
12 T. Nakashima and N. Kimizuka, *Chem. Lett.*, 2002, 1018–1019; J. Hao, A. Song, J. Wang, X. Chen, W. Zhuang, F. Shi, F. Zhou and W. Liu, *Chem. – Eur. J.*, 2005, **11**, 3936–3940; C. R. López-Barrón, D. Li, L. DeRita, M. G. Basavaraj and N. J. Wagner, *J. Am. Chem. Soc.*, 2012, **134**, 20728–20732; F. Gayet, J.-D. Marty, A. Brûlet and N. Lauth-de Viguerie, *Langmuir*, 2011, **27**, 9706–9710; Z. Bai and T. P. Lodge, *J. Am. Chem. Soc.*, 2010, **132**, 16265–16270; R. R. Maddikeri, S. Colak, S. P. Gido and G. N. Tew, *Biomacromolecules*, 2011, **12**, 3412–3417.
13 K. S. Rao, S. Soo and A. Kumar, *Chem. Commun.*, 2013, **49**, 8111–8113.
14 J. N. C. Lopes and A. A. H. Pádua, *J. Phys. Chem. B*, 2006, **110**, 3330–3335; T. S. Kang, K. Ishiba, M. Morikawa and N. Kimizuka, *Langmuir*, 2014, **30**, 2376–2384.
15 S. Javadian, V. Ruhi, A. Heydari, A. A. Shahir, A. Yousefi and J. Akbari, *Ind. Eng. Chem. Res.*, 2013, **52**, 4517–4526.
16 P. Bharmoria, T. J. Trivedi, A. Pabbathi, A. Samanta and A. Kumar, *Phys. Chem. Chem. Phys.*, 2015, **17**, 10189–10199.
17 E. Gómez, B. González, N. Calvar, E. Tojo and Á. Domínguez, *J. Chem. Eng. Data*, 2006, **51**, 2096–2102.
18 D. Otzen, *Biochim. Biophys. Acta*, 2011, **1814**, 562–591.
19 P. D. Ross and S. Subramanian, *Biochemistry*, 1981, **20**, 3097–3102.
20 R. E. M. Diederix, M. Ubbink and G. W. Canters, *Eur. J. Biochem.*, 2001, **268**, 4207–4216.
21 J. A. Laszlo and D. L. Compton, *J. Mol. Catal. B: Enzym.*, 2002, **18**, 109–120.
22 S. P. M. Ventura, L. D. F. Santos, J. A. Saraivab and J. A. P. Coutinho, *Green Chem.*, 2012, **14**, 1620–1625; H. Stamatis, A. Xenakis and F. N. Kolisis, *Biotechnol. Adv.*, 1999, **17**, 293–318; A. Shome, S. Roy and P. K. Das, *Langmuir*, 2007, **23**, 4130–4136.
23 K. Tamura, N. Nakamura and H. Ohno, *Biotechnol. Bioeng.*, 2012, **109**, 729–735.
24 A. Fernández, J. S. Torrecilla, J. García and F. Rodríguez, *J. Chem. Eng. Data*, 2007, **52**, 1979–1983.

